Aalto University

Aaltodoc

OPEN ACCESS

Author(s): Shah, Sahas Bikram & Rasilo, Paavo & Belahcen, Anouar & Arkkio, Antero

Title: Estimation of additional losses due to random contacts at the edges of stator of an electrical machine

Year: 2015

Version: Post print

Please cite the original version:

Shah, Sahas Bikram & Rasilo, Paavo & Belahcen, Anouar & Arkkio, Antero. 2015. Estimation of additional losses due to random contacts at the edges of stator of an electrical machine. COMPEL. Volume 34, Issue 5. 1501-1510. ISSN 0332-1649 (printed). DOI: 10.1108/compel-02-2015-0083.

Estimation of Additional Losses due to Random Contacts at the Edges of the Stator of an Electrical Machine.

Sahas Bikram Shah, Paavo Rasilo, Anouar Belahcen, and Antero Arkkio
Department of Electrical Engineering and Automation, Aalto University, Espoo, Finland
Email: sahas.bikram.shah@aalto.fi

Abstract—The burrs of electrical machine formed during punching process impair the insulation and make random galvanic contacts between the electrical sheets. This paper presents the modeling of random galvanic contacts in a 37 kW induction machine using a surface boundary layer model. Several thousand time stepping finite element simulations were performed, varying the conductivity randomly at the edges of electrical sheets. Then, the additional losses were computed using a vector potential formulation and the surface boundary layer model. The preliminary result showed the increase of total electromagnetic loss by 7.7%

1. Introduction

Electrical steels are usually categorised as grain oriented and non grain oriented. The core losses in non oriented sheets typically range from 0.5 to 2.5 W/kg at 60 Hz and 1.5 T (Ponnaluri, et al., 2001). In such steels, hysteresis loss is dominating which accounts for 60-70 % of the total loss. In grain oriented steels, the typical core loss range from 0.3 to 0.5 W/kg at 60 Hz and eddy current loss are about 75 % of the total loss (Ponnaluri, et al., 2001), (Armco Corporation, 2014). These steels have superior magnetic properties in the rolling direction. Grain oriented and non oriented steels which contain iron silicon are soft magnetic material. This makes them more prone to form burrs when punched depending on the clearance of the blades (Baudouin, et al., 2003). The effect of the burrs on these steels due to punching is studied in (Baudouin, et al., 2003), (Roger, et al., 2009). It has been observed that there is significant heating in the vicinity of the burred region of laminated steels (Mazurek, et al., 2010). Similarly, a few percent of increment in iron losses was observed in (Moses & Aimoniotis, 1989).

In large electrical machines, the burrs formed at the sheets are removed by the deburring process but still the deburring process can introduce some insulation faults and causes galvanic contacts between the sheets (Marion-Pera, et al., 1995). The effect of burrs is also significant in non oriented steels. The formation of the burr at the edge of electrical steels depends on the age of the punching tools and stacking pressure. It was observed in (Arshad, et al., 2007) that the increased iron loss due to the age of punching tool was because of the increased hysteresis loss. In the same study, the pressing of the laminated sheets increased the eddy current loss which suggests that it deteriorates the insulation of adjacent sheets and causes galvanic contacts between the sheets.

There are many studies done to model the inter-laminar short circuit of laminated sheets. These studies are based on both analytical and experimental approach. In (Mazurek, et al., 2012), (Moses & Aimoniotis, 1989) artificial galvanic contacts are applied at the opposite sides of the transformer limbs and additional losses are quantified through measurement. In (Roger, et al., 2009) an analytical approach was considered. Interlaminar shortcircuits of the sheets influenced the impedance of the coil and it was modeled with a permeance network. In (Handgruber, et al., 2013) three dimensional eddy current models were developed to study the interlaminar current in induction machines. The burrs formed at the edges of the sheets are random in nature and introduce uncertainties in the solution. There are studies done in (Ramarotafika, et al., 2012) where uncertainties due to measurement in permeabilities are considered. The interlaminar resistance distribution due to punching is discussed in (Schmidt & Beiler, 1947) which states that losses due to interlaminar currents are no more than one percent of the total core loss.

In this paper, randomness in interlaminar short circuits is addressed by performing several simulations on a 37 kW induction machine. This paper discusses the formulation of a novel surface boundary layer model and its implementation in the 37 kW induction machine to estimate the additional loss due to the random galvanic contact at the edges of the stator

2. Methods and Results

A. Problem study

It is now evident from the literature study that the punching forms the burrs and pressing of the burred sheets causes the random galvanic contacts. The effect of the galvanic contact was first studied in two laminated sheets. The thickness of the sheets is in y direction and breadth of the sheet is in x direction as shown in Figure 1. Magnetic flux density was forced in the z direction using boundary conditions as given by (9). The galvanic contact was placed in the opposite side between the laminated sheets where it deteriorates the insulation. Due to symmetry, the sheets with contact are shown in Figure 2. The study was done in COMSOL solving the following Maxwell's equations,

$$\nabla\times\boldsymbol{E} = -j\omega\boldsymbol{B}, \tag{1}$$

$$\nabla\times\boldsymbol{H} = \boldsymbol{J}, \tag{2}$$

$$\nabla\cdot\boldsymbol{B} = 0. \tag{3}$$

The material equation is given by,

$$\boldsymbol{B} = \mu\boldsymbol{H}, \tag{4}$$

$$\boldsymbol{J} = \sigma\boldsymbol{E}. \tag{5}$$

B and ***H*** are magnetic flux density and magnetic field strength, respectively. The time varying magnetic flux induces the electric field (***E***) and in the presence of a conductor, it produces the current density ***J***. The Maxwell's equation was solved by introducing a vector quantity called the magnetic vector potential (***A***) that can be expressed as,

$$\boldsymbol{B} = \nabla\times\boldsymbol{A} \tag{6}$$

Substituting, (6) in (1) and solving for electric field, the following expression is obtained,

$$\boldsymbol{E} = -\sigma j\omega\boldsymbol{A} - \nabla\phi. \tag{7}$$

Now, (5) can be written as,

$$\boldsymbol{J} = -\sigma j\omega \boldsymbol{A} - \sigma \nabla \phi. \tag{8}$$

ϕ is the scalar potential and the integration of the gradient of the scalar potential is associated with induced voltage. In this problem identification study, magnetic flux density was forced in z direction using boundary conditions.

$$\boldsymbol{B}_z = \left(\frac{\partial \boldsymbol{A}_y}{\partial x} - \frac{\partial \boldsymbol{A}_x}{\partial y} \right) \tag{9}$$

On the boundaries of Figure 2 and Figure 1, the following conditions were applied,

A_x=A_{x1}=constant on Γ_1,

A_x=$-A_{x1}$=constant on Γ_3,

A_y=$-A_{y2}$=constant on Γ_2,

A_y= 0 on Γ_4,

and flux in the sheet is given by,

$$\phi = \int_S \boldsymbol{B}_z ds$$

For the uniqueness of the solution for above mentioned expression, the Coulomb gauge $\nabla \cdot \boldsymbol{A} = 0$ and $\nabla \cdot \left(-\sigma j\omega \boldsymbol{A} - \sigma \nabla \phi \right) = 0$ was enforced.

Table I: Electrical Sheet Parameter

Dimension	90mm x 26 mm x 0.2 mm
Burr width	0.1 mm
Conductivity	3 MS/m

The solutions obtained from solving the above equations are shown in Figure 1 and Figure 2. It can be seen that in the sheets without contact, the time varying flux density induces the current density in each lamination and there is no flow of current from one sheet to the other. However, in the sheets with galvanic contacts, there are induced current density loops in each individual sheet and the bigger loops through the formed contacts. The bigger loops of induced current density are only formed when there is presence of galvanic contacts at both sides.

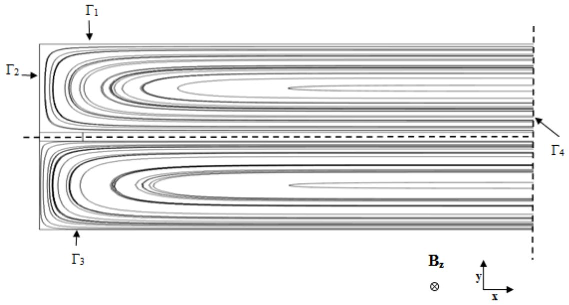

Fig. 1. Induced surface current density with no galvanic contact

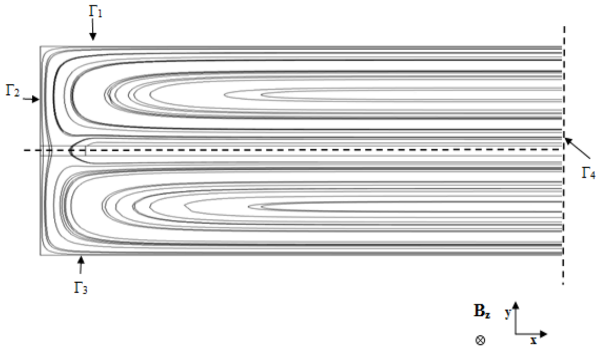

Fig. 2. Induced surface current density with galvanic contact

The objective of the problem study was to observe how the induced current density loops are formed in the presence of the galvanic contacts. The finite element computation of the thin laminated sheet is very expensive. The thin laminated sheets require an extremely fine mesh. This computational limitation allowed only to study the time harmonic and linear material. The eddy current problems in thin laminated sheets are usually studied by reducing the problem size by using homogenization techniques (Krähenbul, et al., 2004) and using anisotropic conductivity (Hollaus & Biro, 1999), basically assigning a low conductivity in the normal direction of the lamination. The analytical modeling of thin electrical sheets including the skin depth is discussed in (Pavo, et al., 2003), (Hamzehbahmani, et al., 2014). The dimensions of the sheets are tabulated in Table I. The thicknesses of the sheets were considered to be greater than the skin depth and the insulation layer was modeled as an air gap.

B. Surface boundary layer model

The above study showed that the galvanic contacts formed by the burrs on the opposite side of the sheets forms additional loops of induced current density. In a two dimension finite element study where the current density is assumed inside or outside the plane, the gradient of scalar potential ($\nabla\varphi$) can be neglected. It is assumed that the length of the conductor beyond the plane is infinitely long and the induced voltage is zero. The presence of the surface current at the edges of sheets causes the discontinuity in the tangential component of the magnetic field.

Table II Machine Parameter

Machine type	Cage Induction
Voltage	400 V
Rated Power	37 kW
Number of Poles	4
Frequency	50 Hz
Rated Slip	0.016

Based on this principle and a vector potential formulation, the surface boundary layer model was developed. The derivation and the explanation of the formulation is given in (Shah, et al., 2013). The surface boundary layer model was compared to an extremely fine mesh and both the models gave similar results. The discontinuity in the tangential component of the magnetic field is given by,

$$\nu_{\mathrm{Fe}} \nabla A \cdot \mathbf{n} - \nu_{\mathrm{air}} \nabla A \cdot \mathbf{n} = \sigma h \frac{\partial A}{\partial t}. \tag{10}$$

The weak form of the formulated equation on iron boundary Γ_{Fe} is given by,

$$\int_{\Omega_{\mathrm{Fe}}} \nu_{\mathrm{Fe}} \nabla A \cdot \nabla w d\Omega + \int_{\Omega_{\mathrm{air}}} \nu_{\mathrm{air}} \nabla A \cdot \nabla w d\Omega - \oint_{\Gamma_{\mathrm{Fe}}} w \sigma h \frac{\partial A}{\partial t} d\Gamma_{\mathrm{Fe}} = 0. \tag{11}$$

The first two parts of the above equation represent the conventional finite element formulation for non conducting iron sheets. The effect of the galvanic contacts at the edges of the sheets on the global solution is obtained by the additional boundary condition which is the third term in (11). The conductivity of the burr and its width is given by σ and h respectively and only the product of those terms matters. The use of the line elements at the edges in the surface boundary layer model reduces the requirement of extremely fine mesh.

3. Results and Discussion

The surface boundary layer model was implemented in house software to study the effect of galvanic contacts on a 37 kW machine. The machine characteristics are shown in Table II. The non linear field equations were coupled to stator and rotor voltage equations (Arkkio, 1987). The time stepping was done using Crank Nicolson method. Two hundred time steps were used per period. Two different cases related to 37 kW induction machine were studied. In the first case, it was assumed that the galvanic contact is formed at the tip of one stator tooth and on the stator frame. In the second case, it was assumed that the random galvanic contacts were formed at all the edges of the stator.

A. Case A: One teeth Burred

The surface boundary layer was implemented at the tip of one stator tooth as shown in Figure 3. The difference of the solutions between one tooth burred machine and healthy machine is shown in Figure 4.

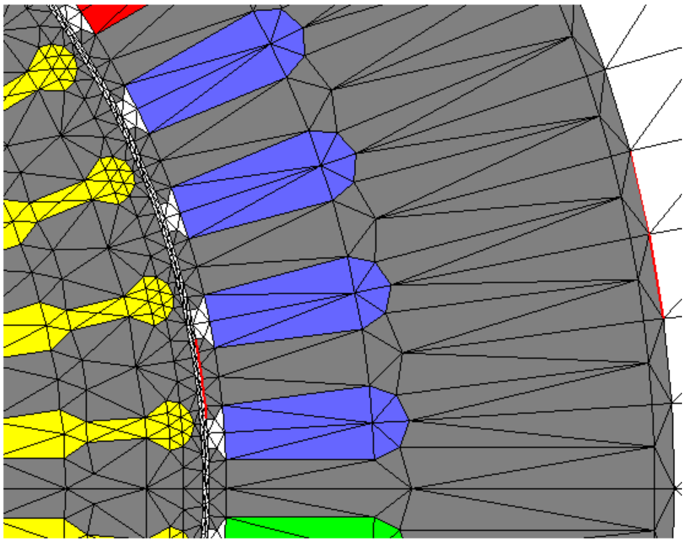

Fig. 3. One teeth burred

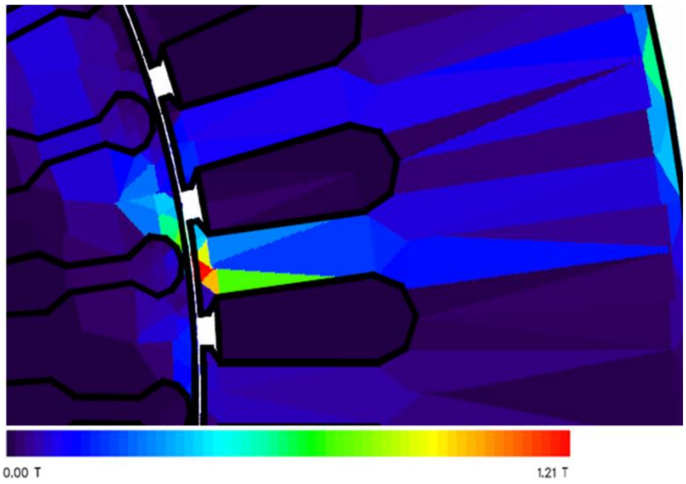

Fig. 4. Flux density difference between healthy and faulty ones

The rotor and stator core losses were compared with the healthy electrical machine. The losses were obtained by varying σh. The stator and rotor loss were compared with the healthy ones. The difference of stator and rotor losses compared to healthy machine's loss is shown in Fig. ***5***. The machine was studied under voltage supply and an additional loss at the stator edges were calculated using (12) and it shows the linear relation with σh. Rotor losses include resistive loss at rotor bar and core loss. Rotor loss does not increase at lower σh but increases significantly at higher σh. The conducting edge at the tip of the stator tooth pushes the flux towards rotor as shown in Fig. ***4***. It is the difference plot of the solution. Hence, the resisitve loss at the rotor cage increases significantly due to higher harmonics of air gap flux that is pushed towards the rotor.

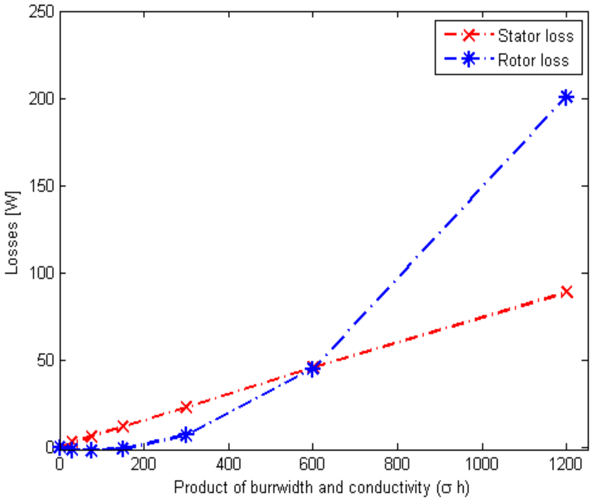

Fig. 5. Total iron loss difference between one tooth faulty and healthy machine

B. Case B: Randomness in galvanic contacts

The randomness of the contacts was studied in the second case. The statistical analysis was performed using a brute force Monte Carlo method. The conductivity of the galvanic contact was considered to have a uniform distribution. It was varied between [0, 3] MS/m and burr width was considered in the range of 1μm. The complete time stepping simulation was performed for 10000 times. In each complete time stepping simulation, random conductivity was assigned at the edges of the stator. This is equivalent as performing simulations on 10000 different machines.

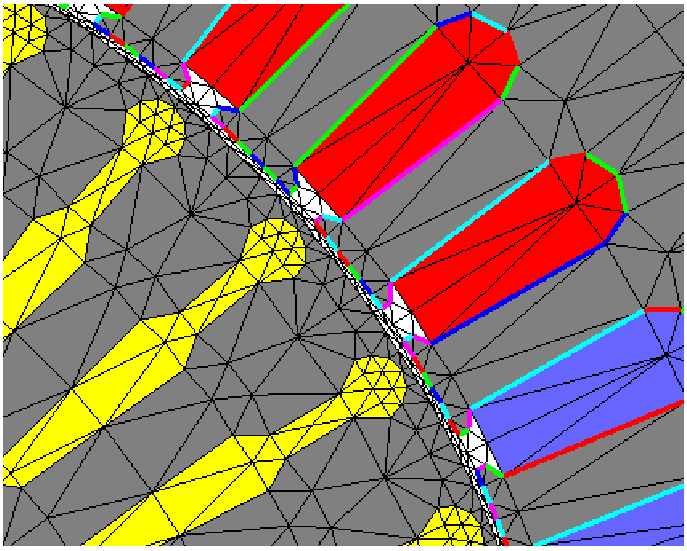

Fig. 6. Different color representation of random conductivity

The air gap torque and losses at stator edges were studied in this paper. The air gap torque was calculated using virtual work method (Arkkio, 1987) for every simulation. The distribution of air gap torque is shown in Figure 7 and it can be seen that the effect of surface boundary layer model on the operation point was negligible.

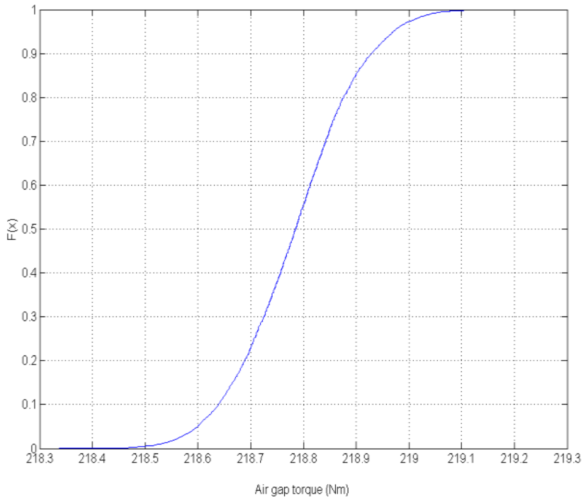

Fig. 7. Cummulative distribution function of computed air gap torque

The losses at the stator edges were computed after each complete time stepping simulation. These losses were computed using (12) where R is the number of the simulations and e is the index of stator edges.

$$P_{\mathrm{add}} = \frac{1}{R}\sum_{n=1}^{R}\left(\frac{1}{\mathrm{T}}\int\int_{\Gamma}\sigma_n^{\ e} h\left(\frac{\partial A(x,y,t)}{\partial t}\right)^2 d\Gamma dt\right) \tag{12}$$

Their cumulative distribution function was obtained and shown in Figure 8. The mean of the computed loss was 193 W and the standard deviation was obtained 16 W. The mean value of total electromagnetic loss was increased by 7.7% due to random contacts at the edges of sheets. It over estimates the losses since the model assumes the laminations are equally burred. However, this is less likely to happen in practical machine but the local heating due to these interlaminar contacts leads to significant insulation damage.

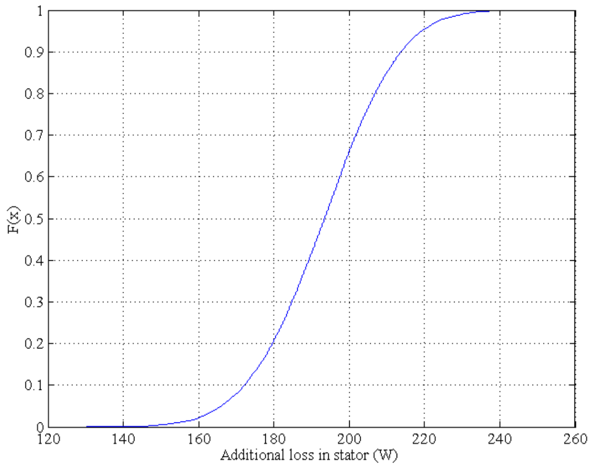

Fig. 8. Cumulative distribution function of computed loss

4. Conclusion

This paper validates the hypothesis of induced current density in burred sheets using finite element method. It also performs the theoretical statistical study of the random conductivity at the stator edge. The surface boundary layer model was implemented in the 37 kW induction machine. The random galvanic contacts at the edges of the stator were addressed by varying the conductivity at the edges and burr width (σh). In future, the conductivity distribution for the laminated sheets will be obtained through rigorous experiment and the obtained results will be compared with stochastic methods.

References

Arkkio, A. (1987), *Analysis of Induction Motors Based on the Numerical Solution of the Magnetic Field and Circuit Equation*, PhD thesis, Helsinki University of Technology, Espoo, Finland.

Armco Corporation (2014), www.armco.com/brochure/product/Electric/Electric.htm. [Online].

Arshad, W. et al. (2007), “Incorporating Lamination Processing and Component Manufacturing in Electrical Design Tools”, *IEEE Industry Applications Conference Record*, pp. 94-102.

Baudouin, P., Wulf, D. M., Kestens, L. & Houbaert, Y. (2003), “The Effect of the Guillotine Clearance on the Magnetic Properties of Electrical Sheets”, *Journal of Magnetism and Magnetic Materials*, Volume 256, pp. 32-40.

Hamzehbahmani, H., Anderson, P., Hall, J. & Fox, D. (2014), “Eddy Current Loss Estimation of Edge Burr Affected Magnetic Lamination Based on Equivalent Network Part I: Fundamental Concepts and FEM modeling”, *IEEE Transaction on Power Delivery*, Volume 29, pp. 642-650.

Handgruber, P., Stermecki, A., Biro, O. & Ofner, G. (2013), “Evaluation of Interlaminar Eddy currents in Induction Machines”, *IECON 2013*, pp. 2792-2797.

Hollaus, K. & Biro, O. (1999.), "Estimation of 3D eddy currents in conducting laminations by an anisotropic conductivity and a 1D analytical model", *COMPEL-The international journal for computation and mathematics in electrical and electronic engineering*, Volume.18(3), pp. 494-503.

Krähenbul, L., Dular, P., Zeidan, T. & Buret, F. (2004), "Homogenization of Lamination Stacks in Linear Magnetodynamics", *IEEE transaction on Magnetics*,Volume 40(2), pp. 912-915.

Marion-Pera, M., Kedous-Lebouc, A., Waeckerle, T. & Cornut, B. (1995), "Characterization of SiFe Sheet Insulation", *IEEE Transaction on Magnetics*, Volume 31, pp. 2408-2415.

Mazurek, R. et al. (2012), "Effect of Artifical Burrs on Local Power Loss in a Three-Phase Transformer Core", *IEEE Transaction on Magnetics*, Volume 48, pp. 1653-1656.

Mazurek, R., Marketos, P., Moses, A. & Vincent, J. (2010), "Effect of Artifical Burrs on the Total Power Loss of a Three Phase Transformer Core", *IEEE Transactions on Magnetics*, Volume 46, pp. 638-641.

Moses, A. & Aimoniotis, M. (1989), "Effect of Artifical Edge Burrs on the Properties of a Model Transformer Core", *Physica Scripta*, Volume 39, pp. 391-393.

Pavo, J., Sebestyen, I., Gyimothy, S. & Biro, O. (2003), "Approximate prediction of losses in transformer plates", *COMPEL-The international journal for computation and mathematics in electrical and electronic engineering*, 22(3), pp. 689-702.

Ponnaluri, S. V., Cherukuri, R. & Molian, P. A. (2001), "Core Loss Reduction in Grain Oriented Silicon Steels by Excimer Laser Scribing: Part I: Experimental Work", *Journal of Materials Processing Technology*, Volume 112, pp. 199-204.

Ramarotafika, R., Benanou, A. & Clenet, S. (2012), "Stochastic Modeling of Soft Magnetic Properties of Electrical Steels:Application to Stators of Electrical Machines", *IEEE Transactions on Magnetics*, Volume 48, pp. 2573-2584.

Roger, J.-Y.et al. (2009), "Electromagnetic Modelling of Short Circuited Core Plates", *COMPEL: The International Journal for Computation and Mathematics in Electrical and Electronic Engineering*, Volume 28, pp. 762-771.

Schmidt, P. & Beiler, A.(1947), "Interlaminar Eddy Current Loss in Laminated Cores", *Transactions of the American Institute of Electrical Engineers*, Volume 66(1), pp. 872-878

Shah, S. B., Rasilo, P., Belahcen, A. & Arkkio, A. (2013), "Modeling of Losses due to Interlaminar Short-Circuit Current in Lamination Stacks", *Electrical, Control and Communication Engineering*, Volume 3(1), pp. 31-36.